

The Impact of Assimilating Additional Dual-Polarimetric Parameters with an LETKF Assimilation System in a Real Summer Case

Kao-Shen Chung¹, Bing-Xue Zhuang¹, Chih-Chien Tsai²

¹Department of Atmospheric Science, National Central University,

²National Science and Technology Center for Disaster Reduction

Abstract

The impact of assimilating dual-polarimetric (dual-pol) parameters is evaluated a real case with squall lines induced by synoptic southwestern wind. WRF-LETKF Radar Assimilation System (WLRAS) is applied to assimilate differential reflectivity (Z_{DR}) and specific differential phase (K_{DP}) in addition to radial wind (V_r) and reflectivity (Z_H) with two different microphysics parameterization (MP) schemes, GCE and MOR. A series of experiments is conducted, and the final analysis in each experiment is applied to initialize the very short-term quantitative precipitation forecast (QPF). The results show that assimilating additional K_{DP} with either GCE scheme or MOR scheme is capable to make the strong convection more intense in the final analysis. In addition, assimilating additional Z_{DR} with GCE scheme corrects the overestimated mean diameter, yet it slightly reduces the intensity of the convective storm. On the other hand, assimilating additional Z_{DR} with MOR scheme modifies the overestimation of Z_{DR} and enhances the signal of strong convection with the value of K_{DP} closer the observation. There is more flexibility to adapt the adjustment obtained from assimilating additional dual-pol parameters in MOR scheme because it predicts both mixing ratio and total number concentration. Through the cross correlation, the assimilated dual-pol parameters can also adjust dynamical fields and thermodynamical fields. It is found that assimilating additional dual-pol parameters can enhance vertical velocity and increase water vapor when the whole assimilation cycles are completed. As a result, one still can see the improvement of QPF by using GCE scheme in the heavy rainfall area. The accumulated rainfall and the probability of heavy rainfall are significantly improved when additional Z_{DR} is assimilated with MOR scheme. With this multi-scale severe weather case study, it is found that multi-moment schemes are more flexible to adjust hydrometeor variables; therefore, if one is intent to assimilate dual-pol parameters in addition to V_r and Z_H , it is more suitable to use multi-moment schemes in the data assimilation system.

Keywords: Dual-Polarimetric Parameters, EnKF

1. Introduction

In radar data assimilation, there have been many studies assimilating V_r and Z_H through either variational method or ensemble Kalman filter (EnKF) to improve the analysis field of severe weather system (Chung et al. 2009; Chang et al. 2014). Because there will be more and more dual-pol radars measuring dual-pol parameters, certain studies try to assimilate dual-pol parameters in addition to V_r and Z_H to make use of the extra information to better capture the structure and location of the precipitation system (Wu et al. 2000; Li and Mecikalski 2010, 2012). Jung et al. (2008a) developed an operator that considers scattering amplitude simulated by T-matrix, hydrometeor and a simple melting model to convert model variables to dual-pol parameters. Jung et al. (2008b) then applied the operator to assimilated simulated dual-pol parameters directly with an EnKF assimilation system in an observation system simulation experiment (OSSE). The result indicates that assimilating additional polarimetric parameters improves the convective scale analysis

especially at the later cycles, and they expected there will be more positive improvement if a more complicated MP scheme is applied. Putnam et al. (2019) first tried to assimilate dual-pol parameters through an EnKF assimilation system with the operator developed by Jung et al. (2010) in a real case with a tornadic supercell. They found that the mesocycle structure is illustrated with the assimilation of Z_{DR} below 2-km height, indicating the relationship between the dual-pol signature and the dynamical process in the convective storm. Tsai and Chung (2020) assimilated dual-pol parameters in the case study of Typhoon Soudelor and found that the performance of the quantitative precipitation forecast (QPF) is improved.

The application of dual-pol parameters has been operational in QPE yet is still in the early stage in data assimilation. There are only few studies assimilating dual-pol parameters in real cases. Therefore, this study selects a case with strong convection to assimilate dual-pol parameters in addition to V_r and Z_H through the sophisticated polarimetric operator with two different

microphysics parameterization (MP) schemes, GCE and MOR. The purposes are 1) investigating the improvement with assimilation of dual-pol parameters in different MP schemes; 2) evaluating the impact on dynamics and thermodynamics with additional assimilation of dual-pol parameters; 3) verifying the improvement in QPF after assimilating additional dual-pol parameters.

2. Case Overview

The case that is selected to conduct assimilation experiments in this study is squall lines observed during the 8th intensive observation period (IOP#8) in the Southwest Monsoon Experiment (SoWMEX) in 2008. Warm and moist air is transported to Taiwan Straits through the strong southwestern wind in the lower level (Figure 1), and the monsoon low in the lower level collocating with the intense short-wave trough in the upper level provides instability in dynamical fields (Figure 2). The unstable synoptic environment induced squall lines over Taiwan Straits (Figure 3). Most of the observed Z_{DR} is lower than 1.0 (Figure 4), which means the mean size of raindrops inside the precipitation system is very small. The intense Z_H results from numerous small raindrops. The 24-hour rainfall accumulation from 0000 LST June 14th 2008 to 0000 LST June 15th 2008 was higher than 90 mm over southwestern Taiwan, and the rainfall maximum exceeded 200 mm (Figure 5).

3. Experiment Design

Weather Research and Forecast (WRF) version 3.9.1 is applied in this study. Figure 6 shows the configuration of three nested domains with 27-km, 9-km and 3-km horizontal resolution respectively. There totally 51 eta levels along the vertical direction with the 10-hPa model top. Two different MP schemes are applied in this study, including GCE and MOR. Initial condition and boundary condition are obtained from NCEP analysis with 1.0° resolution. In order to implement EnKF, the initial condition in D01 and the boundary condition are randomly perturbed through CV3 background error covariance. The perturbed initial condition in D01 will be interpolated to D02 and D03, and there will be ensemble members in all three domains' initial conditions ready for ensemble spin-up and data assimilation.

RCWF, RCCG, RCKT and SPOL (Figure 6) provide the radar observation for data assimilation. These four radars scanned with 9 elevation angles within 7.5 minutes, and SPOL further measured dual-pol parameters, such as Z_{DR} , ρ_{hv} and ϕ_{DP} in addition to V_r and Z_H . Before assimilating the radar data, supperobbing is implemented with Gaussian distance weighting every 5 km in radial direction and every 5° in azimuthal direction for RCWF, RCCG and RCKT; every 4.5 km in radial direction and every 4.5° in azimuthal direction for SPOL.

WRF-LETKF Radar Assimilation System (WLRAS) developed by Tsai et al. (2014) is applied in this study. This assimilation system is based on Local Ensemble Transform Kalman Filter (LETKF) to couple radar

observation and model data. The observation operator based on Jung et al. (2008a) is used to convert model variables to simulated dual-pol parameters. Figure 7 shows the assimilation flow chart. 50 ensemble members are used to conduct the assimilation experiments. After 10-hour spin-up to generate the background field, radar data will be assimilated every 15 minutes from 1000 UTC to 1100UTC. When the assimilation cycling is completed, the analysis field will be applied to initiate the 6-hour ensemble forecast, and then the probability of rainfall accumulation will be calculated based on the ensemble forecast.

Table 1 shows all the updated model variables, localization radius and the inflation factor. In this study, the assimilated observation is allowed to updated all the variables in Table 1. The observation errors set in the experiments are 3 m/s for V_r , 5 dBZ for Z_H , 0.2 dB for Z_{DR} and 0.5°/km for K_{DP} (Jung et al. 2008b; Tsai and Chung 2020). Z_{DR} and K_{DP} will not be assimilated if the altitude is higher than 4-km height. Negative Z_{DR} and K_{DP} are eliminated to satisfy the assumption that larger raindrops are more oblate. Table 2 lists all the experiments in this study. Scheme_VrZ is the control run to investigate the impact of assimilating dual-pol parameters in addition to V_r and Z_H .

4. Results and Discussions

The data inside the black rectangle in Figure 3 is used to plot the contour frequency by altitude diagram (CFAD). CFADs can present the data distribution along the vertical direction in a specific region. Assimilating additional Z_{DR} with GCE scheme makes Z_{DR} quartiles smaller and closer to the observation (Figure 8h), which indicates that the mean size of raindrops is corrected. However, the intensity of the precipitation system becomes weaker with smaller quartiles of Z_H and K_{DP} (Figure 8g,i). When K_{DP} is assimilated in, there is no obvious difference in the CFADs of Z_H and Z_{DR} (Figure 8j,k) comparing with GCE_VrZ, but the value of the 3rd quartile of K_{DP} is higher (Figure 8l), which means the strong convection is enhanced. When both Z_{DR} and K_{DP} are assimilated with GCE scheme, the result is similar to GCE_VrZZdr, yet the 3rd quartile of K_{DP} is higher. Assimilating additional Z_{DR} with MOR scheme modifies the overestimated Z_{DR} quartiles (Figure 9h) and does not make the intensity of the precipitation system weaker (Figure 9g); Moreover, the 2nd and the 3rd quartiles are larger than MOR_VrZ. Similar to the result of the experiments with GCE scheme, assimilating additional K_{DP} does not show significant difference in the CFADs of Z_H and Z_{DR} while the quartiles of K_{DP} in MOR_VrZKdp is larger than MOR_VrZ. With the additional assimilation of both Z_{DR} and K_{DP} , the value of the 3rd quartile of K_{DP} is even higher, and the CFADs of Z_H and Z_{DR} is similar to MOR_VrZZdr.

The feature of EnKF is updating the background field through the background error covariance (correlation), so the dual-pol parameters are allowed to update dynamical fields and thermodynamical fields via the cross correlation. Figure 10 and Figure 11 are the difference of analysis

mean between experiments with additional assimilation of dual-pol parameters and experiments without it at the final cycle. Although the intensity of the precipitation system is weaker from the view of Z_H in GCE_VrZZdr, there are positive water vapor difference, positive vertical velocity difference and negative divergence difference (Figure 10a,b,c). It seems that the weighting of assimilated Z_{DR} is higher than assimilated K_{DP} that the pattern of the difference in GCE_VrZZK (Figure 10g,h,i) is almost the same as that in GCE_VrZZdr (Figure 10a,b,c). As for the experiments with MOR scheme, the water vapor increases much more significantly in MOR_VrZZdr (Figure 11a) comparing with GCE_VrZZdr. It might result from that MOR tends to simulate raindrops with larger mean diameter. Therefore, the innovation of Z_{DR} will be much higher than other dual-pol parameters. Same as the experiment with GCE, the impact of assimilated Z_{DR} dominates when both Z_{DR} and K_{DP} are assimilated (Figure 11g,h,i).

The final analysis is applied to run the ensemble forecast, and the probability of 6-hour accumulated rainfall exceeding 30-mm is calculated. The precipitation system becomes weaker from the view of Z_H in the final analysis of GCE_VrZZdr, yet the probability of heavy rainfall is higher than GCE_VrZ (Figure 12a,b). It might result from the increase water vapor and enhanced vertical velocity which help to reconstruct the precipitation system when the numerical model starts to integrate. The probability is the highest when both Z_{DR} and K_{DP} are assimilated in GCE_VrZZK and MOR_VrZZK (Figure 12d and Figure 13d), and the probability maximum collocates with the observed heavy rainfall. Therefore, assimilating additional dual-pol parameters can improve the performance of short-term QPF, especially heavy rainfall.

5. Conclusions

This study applies an EnKF assimilation system, WLRAS, to assimilate dual-pol parameters in addition to V_r and Z_H . The purposes are 1) investigating the improvement with assimilation of dual-pol parameters in different MP schemes; 2) evaluating the impact on dynamics and thermodynamics with additional assimilation of dual-pol parameters; 3) verifying the improvement in short-term QPF after assimilating additional dual-pol parameters.

Through the verification with dual-pol parameters, it is found that there is certain limitation in assimilating dual-pol parameters in addition to V_r and Z_H with GCE scheme (a single moment scheme). Single moment schemes only predict mixing ratio, so simulated dual-pol parameters are only determined by mixing ratio. Three simulated dual-pol parameters, Z_H , Z_{DR} and K_{DP} proportional to each other with the implementation of single moment schemes. Therefore, when additional Z_{DR} is assimilated to modify the overestimated Z_H and K_{DP} will also be reduced, which is the limitation of single moment schemes in assimilating dual-pol parameters. On the contrary, MOR scheme (a double moment scheme) shows

some flexibility to adjust the microphysical states with assimilation of dual-pol parameters because it predicts not only mixing ratio but also total number concentration. As a result, assimilating additional Z_{DR} with MOR scheme is capable to reduce the error of all the dual-pol parameters at the same time.

Although assimilating additional Z_{DR} with GCE scheme might make the precipitation system weaker, it can enhance the vertical velocity and increase the water vapor through the cross correlation, which might help to reconstruct the strong convection when model integration starts. There is much more water vapor adjustment in MOR_VrZZdr than GCE_VrZZdr because of the exaggerated overestimation of Z_{DR} in MOR scheme. With the adjustment in dynamical fields and thermodynamical fields, the probability of heavy rainfall in GCE_VrZZdr is still higher than GCE_VrZ, and the probability becomes much higher if both Z_{DR} and K_{DP} are assimilated. As a result, assimilating Z_{DR} or K_{DP} is capable to improve the performance of heavy rainfall forecasts.

To summarize all the results mentioned in this study, multi-moment MP schemes shows more flexibility of adjusting the microphysical states in the analysis field when additional dual-pol parameters are assimilated; moreover, the performance of short-term QPF is improved significantly. Therefore, a multi-moment MP scheme is a more suitable option than a single moment scheme if one is intent to assimilate dual-pol parameters in addition to V_r and Z_H .

References

- Chang, W., K.-S. Chung, L. Fillion, and S.-J. Baek, 2014: Radar Data Assimilation in the Canadian High-Resolution Ensemble Kalman Filter System: Performance and Verification with Real Summer Cases. *Monthly Weather Review*, **142**, 2118-2138.
- Chung, K.-S., I. Zawadzki, M. K. Yau, and L. Fillion, 2009: Short-Term Forecasting of a Midlatitude Convective Storm by the Assimilation of Single-Doppler Radar Observations. *Monthly Weather Review*, **137**, 4115-4135.
- Jung, Y., G. Zhang, and M. Xue, 2008a: Assimilation of Simulated Polarimetric Radar Data for a Convective Storm Using the Ensemble Kalman Filter. Part I: Observation Operators for Reflectivity and Polarimetric Variables. *Monthly Weather Review*, **136**, 2228-2245.
- Jung, Y., M. Xue, G. Zhang, and J. M. Straka, 2008b: Assimilation of Simulated Polarimetric Radar Data for a Convective Storm Using the Ensemble Kalman Filter. Part II: Impact of Polarimetric Data on Storm Analysis. *Monthly Weather Review*, **136**, 2246-2260.
- Jung, Y., M. Xue, and G. Zhang, 2010: Simulations of Polarimetric Radar Signatures of a Supercell Storm Using a Two-Moment Bulk Microphysics Scheme. *Journal of Applied Meteorology and*

Climatology, **49**, 146-163.

- Li, X., and J. R. Mecikalski, 2010: Assimilation of the dual-polarization Doppler radar data for a convective storm with a warm-rain radar forward operator. *JGR Atmospherics*, **115**.
- Li, X., and J. R. Mecikalski, 2012: Impact of the Dual-Polarization Doppler Radar Data on Two Convective Storms with a Warm-Rain Radar Forward Operator. *Monthly Weather Review*, **140**, 2147-2167.
- Putnam, B., M. Xue, Y. Jung, N. Snook, and G. Zhang, 2019: Ensemble Kalman Filter Assimilation of Polarimetric Radar Observations for the 20 May 2013 Oklahoma Tornadoic Supercell Case. *Monthly Weather Review*, **147**, 2511-2533.
- Tsai, C.-C., S.-C. Yang, and Y.-C. Liou, 2014: Improving quantitative precipitation nowcasting with a local ensemble transform Kalman filter radar data assimilation system: observing system simulation experiments. *Tellus A*, **66**, 21804.
- Tsai, C.-C., and K.-S. Chung, 2020: Sensitivities of Quantitative Precipitation Forecasts for Typhoon Soudelor (2015) near Landfall to Polarimetric Radar Data Assimilation. *Remote Sensing*, **12**, 3711.
- Wu, B., J. Verlinde, and J. Sun, 2000: Dynamical and Microphysical Retrievals from Doppler Radar Observations of a Deep Convective Cloud. *Journal of the Atmospheric Sciences*, **57**, 262-283.

Table 1 Localization radius and inflation factor for each model variables.

	U · V	W	PH · T	Qv · Qc · Qt · Nc · Ni	Qr · Qs · Qg · Nr · Ns · Ng
Horizontal localization radius (km)	36	12	12	24	12
Vertical localization radius (km)	4				
Inflation	1.08				

Table 2 All the experiments in this study.

	V _r	Z _H	Z _{DR}	K _{DP}
Scheme_VrZ	V	V		
Scheme_VrZZdr	V	V	V	
Scheme_VrZKdp	V	V		V
Scheme_VrZZK	V	V	V	V

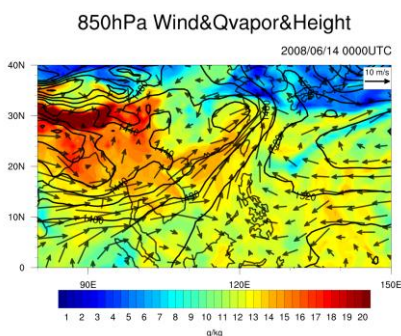


Figure 1 Wind field, water vapor mixing ratio (shaded) and geopotential height (contour) of NCEP analysis at 850 hPa at 0000 UTC 14th June 2008.

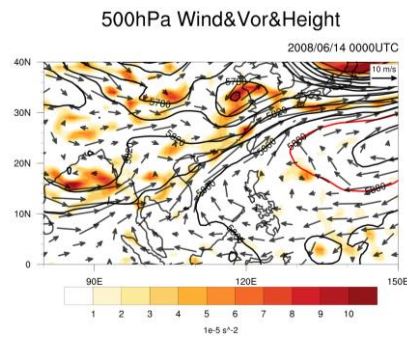


Figure 2 Wind field, relative vorticity (shaded) and geopotential height (contour) of NCEP analysis at 500 hPa at 0000 UTC 14th June 2008. Red contour is 5880-meter geopotential height.

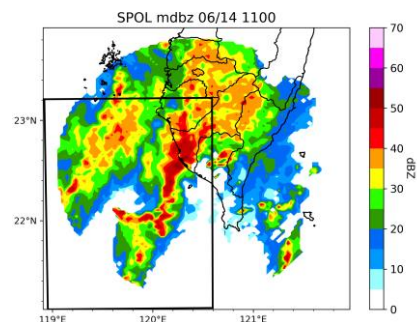


Figure 3 Composite Z_H maximum observed by SPOL at 1100 UTC 14th June 2008. The radar data inside the black rectangle is used to plot CFADs.

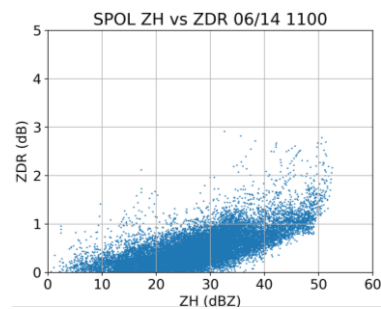


Figure 4 Scatter plot of Z_H and Z_{DR} observed by SPOL below 4-km height at 1100 UTC 14th June 2008.

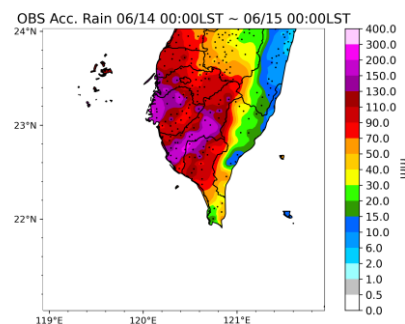


Figure 5 Accumulated rainfall from 0000 LST 14th June 2008 to 0000 LST 15th June 2008. Black dots show the location of CWB observation sites.

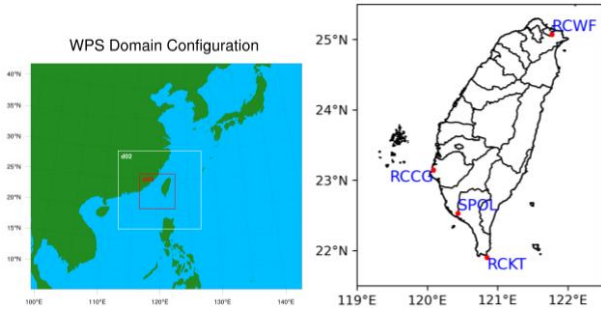


Figure 6 Domain configuration and the location of RCWF, RCCG, RCKT and SPOL.

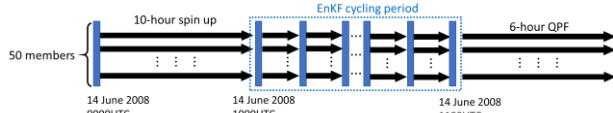


Figure 7 Assimilation flow chart.

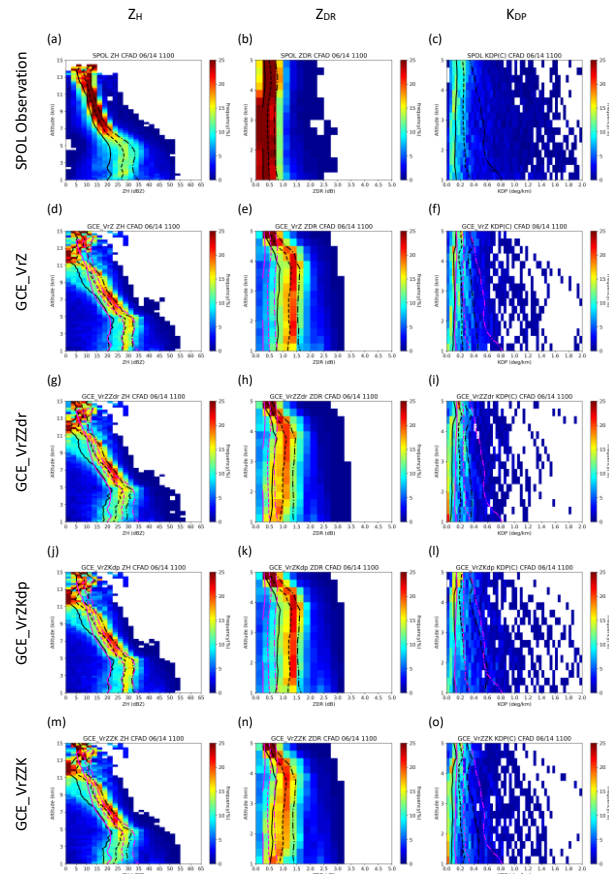


Figure 8 Dual-pol parameter CFADs of SPOL observation and the experiments with GCE scheme at 1100 UTC 14th June 2008. The pink lines are the accumulated 25%, 50% and 75% of SPOL observation.

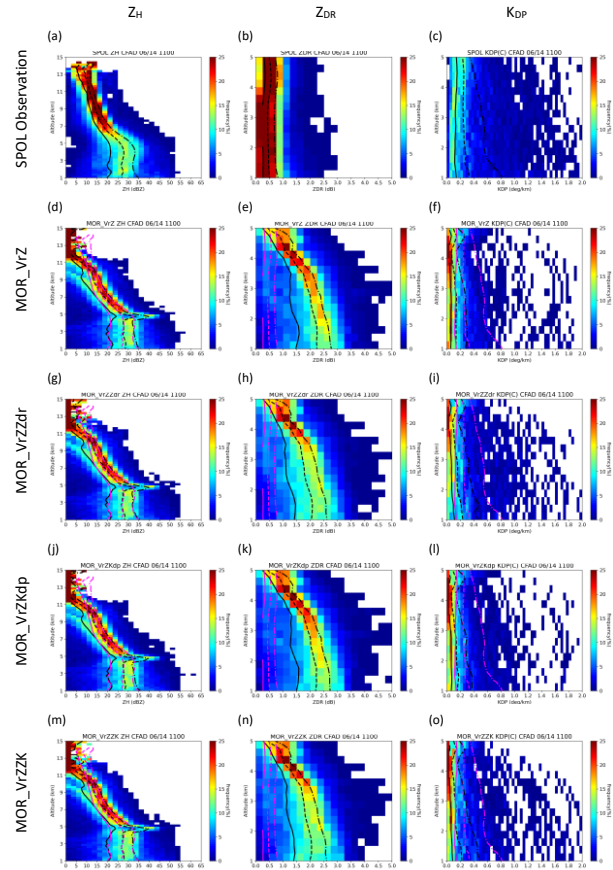


Figure 9 Dual-pol parameter CFADs of SPOL observation and the experiments with MOR scheme at 1100 UTC 14th June 2008. The pink lines are the accumulated 25%, 50% and 75% of SPOL observation.

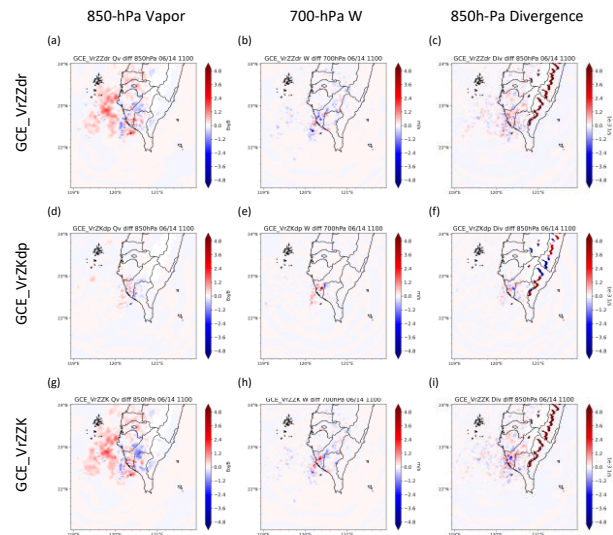


Figure 10 Analysis mean difference of 850-hPa water vapor, 700-hPa vertical velocity and 850-hPa divergence in the experiments with GCE scheme at 1100 UTC 14th June 2008. GCE_VrZ is the reference.

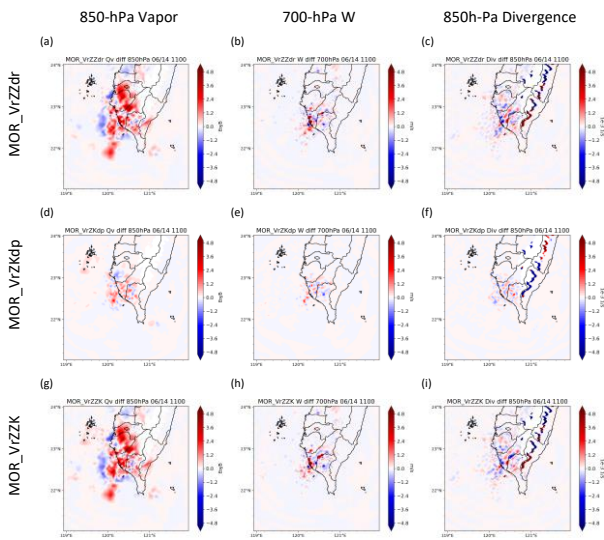


Figure 11 Analysis mean difference of 850-hPa water vapor, 700-hPa vertical velocity and 850-hPa divergence in the experiments with MOR scheme at 1100 UTC 14th June 2008. MOR_VrZ is the reference.

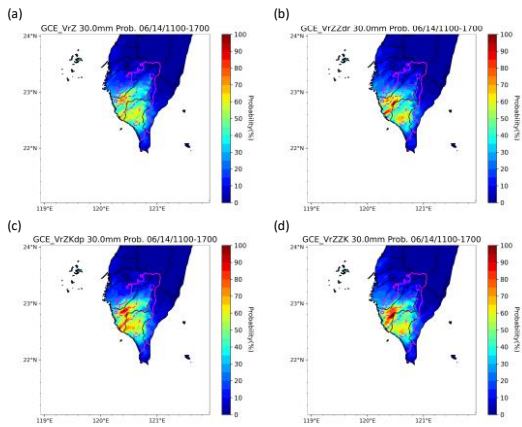


Figure 12 Probability of 6-hour accumulated rainfall exceeding 30 mm in the experiments with GCE scheme. The solid contour and the dashed contour represent 30-mm and 60-mm contours respectively.

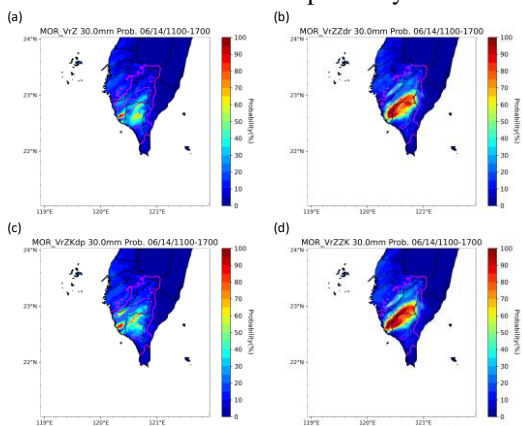


Figure 13 Probability of 6-hour accumulated rainfall exceeding 30 mm in the experiments with MOR scheme. The solid contour and the dashed contour represent 30-mm and 60-mm contours respectively.